ISSN 1063-7842, Technical Physics, 2016, Vol. 61, No. 9, pp. 1303–1311. © Pleiades Publishing, Ltd., 2016.
Original Russian Text © M.V. Piskunov, P.A. Strizhak, 2016, published in Zhurnal Tekhnicheskoi Fiziki, 2016, Vol. 86, No. 9, pp. 24–31.

GASES AND LIQUIDS

Difference in the Conditions and Characteristics of Evaporation of Inhomogeneous Water Drops in a High-Temperature Gaseous Medium

M. V. Piskunov* and P. A. Strizhak

National Research Tomsk Polytechnic University, pr. Lenina 30, Tomsk, 634050 Russia

**e-mail: piskunovmv@tpu.ru*

Received October 5, 2015; in final form, February 2, 2016

Abstract—The evaporation of water drops of initial mass 5–15 mg on a stationary graphite substrate, as well as inhomogeneous drops with solitary solid inclusions, during heating by high-temperature combustion products has been investigated experimentally. Experiments have also been carried out with analogous inhomogeneous drops moving through combustion products. The possibility of two mechanisms of phase transformations of inhomogeneous liquid drops has been established. The scales of the effect of the area of the inclusion surface (up to 20%) and the initial mass of water (up to 90%) on the characteristics of the evaporation of inhomogeneous drops have been determined.

DOI: 10.1134/S106378421609019X

INTRODUCTION

As a rule, the introduction (addition) of specialized solid inclusions (particles) into liquids, emulsions, and suspensions (with the corresponding spraying of the latter materials) is mainly aimed at intensifying [1–5] phase transformations at the inner and outer boundaries of liquid–gas and liquid–solid interfaces. The results of theoretical [1, 2] and experimental investigations [3–5] illustrate bright prospects (increase in the efficiency of using water management [6]) of applying this approach in thermal power engineering, chemical and petrochemical industries, fire and explosion safety, and so on.

It should be noted that the mechanism of phase transformations at the solid particle–water interface in an inhomogeneous drop has been investigated insufficiently. It is expedient to pay special attention to determining the dominating mechanism of phase transformations during the interaction of water drops with solid inclusions in a high-temperature (about 1100 K) gaseous medium and to determine the conditions for realizing various regimes of evaporation. The solution of this problem will make it possible to use this approach to intensify phase transformations in a wide range of applications (e.g., thermal or fire treatment of technological sewage and waste water [7]; polydisperse firefighting [8]; obtaining heat-transfer agents based on combustion gases, water drops, and vapor [9]; unfreezing loose media [10], and treating slagged heat-loaded surfaces of power equipment [11]).

As a result of theoretical and experimental investigations [12], it was found that there are several mechanisms of the evaporation of a liquid drop containing a commensurate opaque inclusion, i.e., the evaporation of liquid with the free (outer) surface of a drop and boiling on the inner interface between media, which leads the explosive destruction of the drop. We can also note the results of investigations of the evaporation of liquid drops on substrates made of various materials (see, e.g., [13–16]). These experiments are analogous (as regards the methods employed) to those in [12]. The results of these experiments are in good agreement with the experimental data obtained in [3–5, 17]. An analysis of the results obtained in [12–17] leads to the conclusion that, among parameters of phase transformations, the most significant characteristics mainly determine the course of the process, e.g., the temperature of the gaseous medium and the size and shape of inclusions. It is expedient to experimentally investigate the difference in the conditions and characteristics of evaporation of drops (with single commensurate inclusions) that move through high-temperature gases, stationary inhomogeneous drops on an evaporating substrate (for its size is much larger than that of inclusions).

This study aims at experimental investigation of differences in the conditions and parameters of the processes of evaporation and boiling of inhomogeneous water drops in a high-temperature gaseous medium.

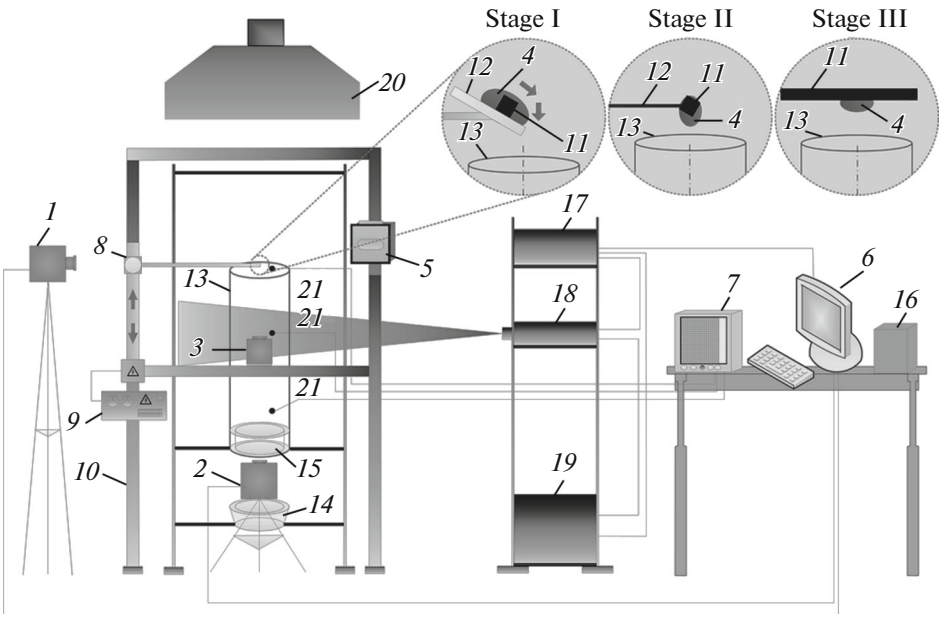

Fig. 1. Schematic diagram of experimental setup: (*1*, *2*) high-speed video cameras; (*3*) cross-correlation chamber; (*4*) water drop; (*5*) illuminating projector; (*6*) personal computer (PC); (*7*) multichannel technological recorder (MTR); (*8*) motorized coordinated device (MCD); (*9*) power supply; (*10*) aluminum holder; (*11*) solid inclusion/graphite substrate; (*12*) substrate with hydrophobic surface/ceramic rod; (*13*) quartz glass cylinder; (*14*) drop catcher; (*15*) hollow cylinder with combustible liquid; (*16*) analytic balance; (*17*) synchronizer of PC, cross-correlation chamber, and laser; (*18*) double pulsed Nd : YAG laser; (*19*) generator of laser radiation; (*20*) pressure system; (*21*) thermocouples.

1. EXPERIMENTAL SETUP AND TECHNIQUES

The experiments were carried out on the setup shown in Fig. 1, which is analogous in the main elements and characteristics to those used in experiments in [12]. The experimental data were processed using the optical method of particle image velocimetry (PIV) [18–20] and Tema Automotive software [12, 21–23].

We prepared graphite particles (inclusions) *11* in the form of cylindrical disks (diameter 1.65 mm, height 3.1 mm), cubes (length, width, and height 1.9 mm), and parallelepipeds (length 1.3 mm, width 1.5 mm, and height 3.5 mm). The particles were weighed using Vibra AF 225DRCE measuring system *16*.The maximal and minimal masses are 220 and 0.001 g, and the error did not exceed 0.5% of the mass being measured. The choice of the inclusions with different configurations was dictated by the need to ensure close areas (which played the role of variable parameters in the experiments) of the surfaces of the resultant inhomogeneous drops and liquid–gas and liquid–solid interfaces.

The high-temperature gaseous medium was generated using denaturated alcohol. The composition of its combustion products included 4.433% CO_2, 0.058% CO, 14.907% O_2, 0.002% NO, 0.002% NO_x, and 80.598% of other hydrocarbon components and N_2. The concentration of the components of combustion products was measured using the Testo 300XXL gas analyzer (±0.2% error and 0.01% measurement resolution). Methyl alcohol (200 mL in volume) was poured into burner *15* (special hollow cylinder) installed at the base of cylindrical channel *13* (analogous to that used in experiments [12]). Then, the burning of alcohol was initiated. Combustion products entered the inner cavity of cylinder *13*. The stabilization of the gas temperature (1100 K) in the channel took 180–210 s. After this time delay, experiments with inhomogeneous water drops began, the temperature T_g of the combustion products was measured using three tungsten–rhenium thermocouples *21* (the measured temperature range was 0–2473 K and the maximal admissible error was $\pm 0.005|T_g|$) fixed at heights of 0.25, 0.5, and 0.75 m (relative to burner *15*). The readings of thermocouples *21* were fed to monitor *7* with subsequently data processing (when required) on personal computer (PC) *6*.

The temperature of the combustion products varied over the cross section of channel *13* in the range of 15–20 K. We detected the change in the temperature over the longitudinal (from the base of the burner to the upper edge of cylinder *13*) section by 18–30 K relative to 1100 K. As a result, in an analysis of the experimental results, we assumed that, on average, the temperature of combustion products in channel *13* was 1100 K.

The PIV method was used to monitor the velocities u_g of the flow of high-temperature gases. The method

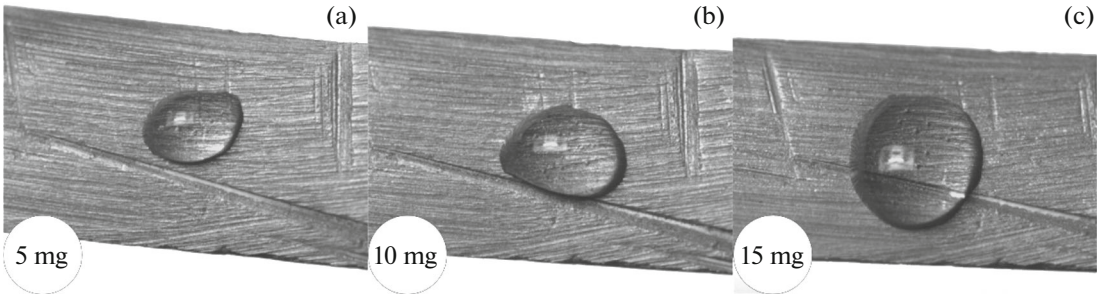

Fig. 2. Water drops (with different initial masses) on the graphite substrate: (a) 5, (b) 10, and (c) 15 mg.

is based on recording the instantaneous velocity distributions of tracer velocities in the gas flow between bursts of laser *18*. The tracer particles (of nanopowder of titanium dioxide TiO_2) were injected into the gas flow at the lower part of cylinder *13* (analogously to experiments in [4, 5, 12]). After control measurements of u_g, the injection of tracers was terminated, and the main experiments with water drops were performed. In all experiments, the velocity of gases was about 1.5 m/s (the velocity was controlled by pressure system *20*).

The experimental technique consisted of several stages. At the first stage (see Fig.1), we recorded images of water drops *4* with graphite inclusions *11* during their motion through quartz cylinder *13* (height 1 m, inner diameter 0.2 m) filled with high-temperature combustion products. The formation and injection of a water drop into cylinder *13* was performed using substrate *12* with a hydrophobic surface (we used paraffin, i.e., octadecane $C_{18}H_{38}$, as the substrate). Water drop *4* was generated by a dispenser (dosage range 10–100 μL, maximal error ±3%) and deposited on substrate *12*. Single inclusion *11* was introduced into drop *4*. Then, substrate *12* was lifted to a height of 1.3 m relative to the base of cylinder *13* by motorized coordinated device *8*, and an inhomogeneous drop was injected into the high-temperature gas.

The Tema Automotive software was used to measure the radii of inhomogeneous drops [1]. Having determined the radii of the drops, we calculated parameter ΔR ($\Delta R = R_0 - R$, where R_0 and R are the radii of a drop before and after its passage through high-temperature combustion products, respectively). Having measured the masses of inhomogeneous liquid drops (using measuring system *16*) before (m_{w0}) and after (m_w) their passage through high-temperature gases, we calculated parameter Δm_w ($\Delta m_w = m_{w0} - m_w$), which characterizes the decrease in the mass of water drop *4*. The mass of inclusion *11* was measured before its introduction into a water drop.

At the second stage of experiments, we studied the evaporation conditions in which an inhomogeneous drop was fixed (using the technique analogous to that in [12]) on ceramic rod *12* (length 0.25 m). On the symmetry axis of inclusion *11*, a technological hole of radius 0.5 mm and a depth not exceeding 0.3 mm was drilled, which made it possible to fix particle *11* on rod *12*. This approach made it possible to control the time of drop heating, and the use of ceramic rod *12* minimized its effect on the occurring thermal processes. Coordinate device *8* moved rod *12* with an inhomogeneous drop fixed on it into channel *13* through the third technological hole (by 0.75 m relative to the burner). In each experiment, video recording continued up to the complete evaporation of water, and lifetimes τ_h of the drops were determined.

The third stage (see Fig. 1) is analogous in all characteristics to the second stage (except for measurements in the rod–inhomogeneous drop system). In particular, rod *12* was replaced by graphite substrate *11* (length 0.1 m, thickness 0.005 m, width 0.01 m). A drop was generated by the dispenser and was placed on the substrate surface (Fig. 2), which was then moved to cylinder *13*.

At each stage, at least ten experiments were performed under identical conditions (initial sizes and masses of drops, temperature of combustion products, and their velocities). The maximal error of calculating the times to the complete evaporation of drops did not exceed 0.005 s. The maximal systematic errors of instruments for measuring the sizes of drops and inclusions were 0.05 mm. Random errors in determining these parameters did not exceed 8–10% relative to the average value for a series.

2. RESULTS AND DISCUSSION

Our experiments have made it possible to determine the main mechanisms and time characteristics of phase transformations for each of the above positions of the interfaces between liquid–gas and liquid–solid interfaces.

Figure 3 shows the typical stages of intense evaporation of a water drop of mass 15 mg on the substrate. We determined the heating times typical of each stage. It should be noted that this variant is characterized by the intense formation of a vapor layer near the liquid–solid interface. It can be seen from Figs. 3a and 3c that the size of a water drop did not noticeably decrease

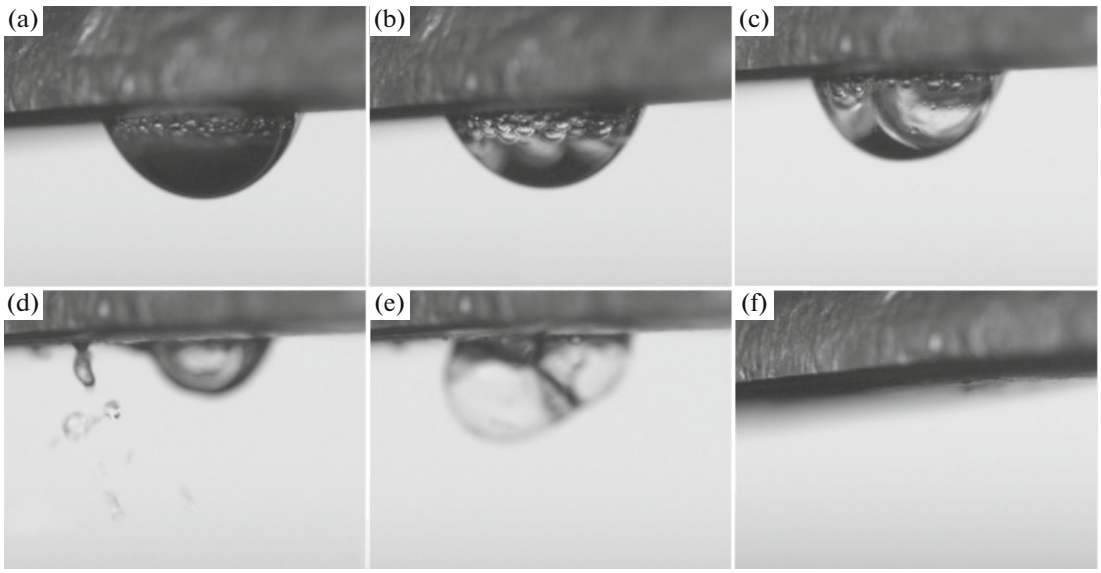

Fig. 3. Photographs of a drop (of mass 15 mg) during its evaporation and boiling on the substrate: (a) $\tau = 0$, (b) 8.20, (c) 12.50, (d) 20.20, (e) 20.54, and (f) 25.65 s.

over heating time $\tau_h \approx 12.5$ s, and the vapor layer filled almost its entire inner cavity during this time interval. In the features of the formation of the vapor layer (Figs. 3a–3c), we can single out the instantaneous (less than 1 s since the beginning of heating) formation of vapor bubbles (as well as their coalescence, coarsening, and detachment) near the inner solid–liquid interface. The predominant mechanism of phase transformation in this case is the intense evaporation at the substrate–liquid interface. Evaporation was hardly observed from the outer surface of the drop. Figure 3d illustrates a certain displacement (relative to the initial position) of a water drop due to an increase in the size of the vapor layer and the separation of liquid fragments (groups of droplets) after the destruction of the film caused by the critical growth of vapor bubbles. The latter process is the result of achieving the conditions under which the pressure of vapor in the drop exceeds the pressure due to surface tension of the liquid and the external medium. In turn, the displacement can be explained by the Leidenfrost effect [24–26]. The formed vapor layer with a lower thermal conductivity [27] as compared to water is a sort of a heat-insulating interlayer (buffer zone) that reduces the area of contact between the liquid and substrate and ensures the slip of the drop. This stage (Figs. 3d and 3e) is characterized by the frequently repeated disintegration of vapor bubbles accompanied by the separation of liquid fragments (Fig. 3f).

The typical stages of realizing several mechanisms of phase transformation (boiling and evaporation) are illustration in Fig. 4. In the given case, the experiment was carried out in accordance with the technique of the second stage. No features of intense vaporization like those in the case with the substrate (see Figs. 3a–3c) are observed at the inclusion–water interface in Figs. 4a–4c for the corresponding times. It can be seen from Fig. 4a that the inclusion is completely covered by liquid. We can state that the layer of liquid is initially heated, and only then is it involved the solid inclusion in heating (in contrast to the case with the substrate, in which its contact with the gas is ensured). The heating of the liquid layer is obviously (see Figs. 4a–4c) accompanied by the evaporation from the outer surface of the drop. At $\tau_h \approx 7.5$ s (see Fig. 4c), the characteristic size of the drop becomes much smaller than its initial size. The amount of energy accumulated by the inclusion at the interface between the media increases significantly when the characteristic thickness of the water film around the inclusion decreases (several faces of the inclusion at this instant are coated only by a thin film of the liquid). In this case, evaporation in the drop is substantially intensified. The process further evolves analogously to the heating of the drop on the substrate (see Figs. 3d–3f); the boiling of the liquid is accompanied by the destruction of the water film.

It should be emphasized that, in the case of the evaporation of a water drop from the substrate, the major role in achieving the conditions of intense evaporation at the interface between the media is played, not by the high temperature of the gaseous medium, but by the large size of the graphite substrate compared to the drop size. During the simultaneous heating of the substrate and the liquid (in contrast to the case depicted in Fig. 4a), a substantial transfer of the energy accumulated by the substrate to the internal solid–liquid interface is ensured due to the high thermal conductivity of graphite compared to that of water [28].

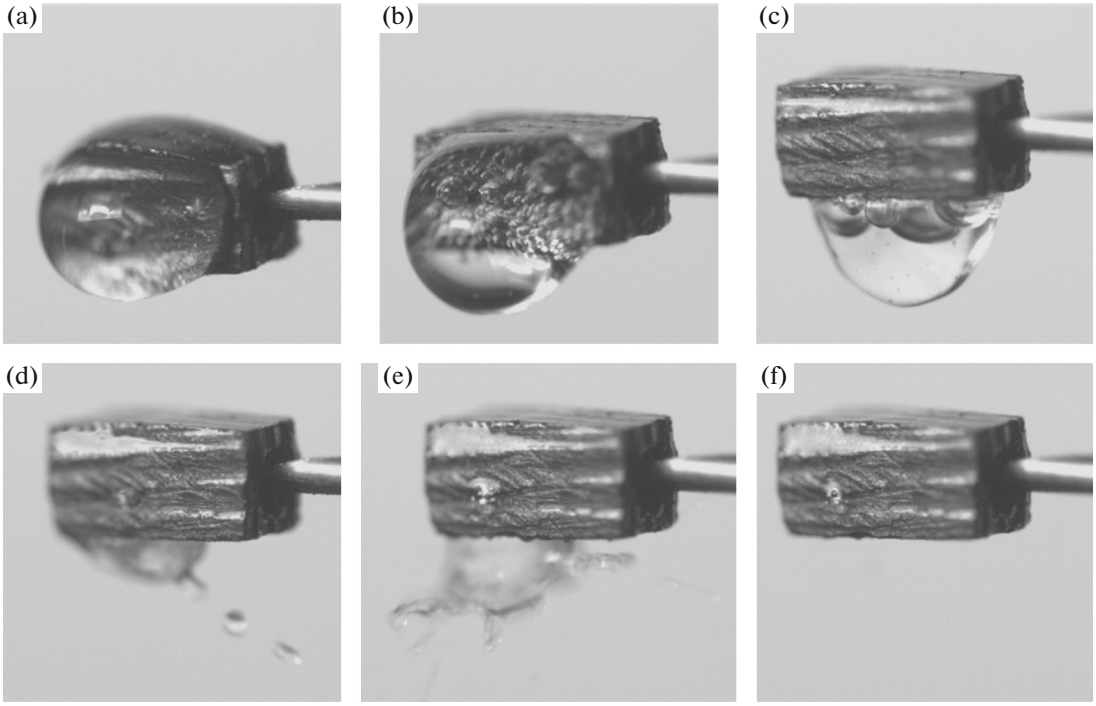

Fig. 4. Photographs of an inhomogeneous drop (of mass 5 mg) fixed on a ceramic rod during its evaporation and boiling: (a) τ = 0, (b) 1.25, (c) 7.47, (d) 12.56, (e) 13.52, and (f) 13.83 s.

Figure 5 shows the results of comparing the lifetime τ_h (time of complete evaporation) of water drops on the substrate (curve *1*) and the inhomogeneous drops with solid inclusions of different sizes (4 mm, curve *2*; 3 mm, curve *3*; and 2 mm, curve *4*) under identical heating conditions. For inhomogeneous water drops (curves *2*–*4*), it can be concluded that the value of τ_h decreases substantially with increasing surface area of the inclusion. The larger the area of the inclusion surface, the larger the amount of energy that accumulates on it after its passage through the layer of the liquid (due to radiant, convective, and conductive heat flows). In view of the opaqueness of the inclusion, the radiant flow is accumulated on the surface of the inclusion after its passage through water (in a thin surface layer). Upon an increase in the area of the contact between the inclusion and the layer of the liquid, the transfer of the thermal energy accumulated by it to the above-mentioned surface layer intensifies. Intense evaporation is observed at the liquid–inclusion interface. The evaporation rates at the inner and outer interfaces between the media increase. It should be noted that, upon an increase in the mass of water, following an inhomogeneous drop from 5 to 15 mg, the complete evaporation time almost doubles (see Fig. 5). It was found that the variations in τ_h for a water drop that evaporates on the substrate is smaller. The lifetime of the drop changes only by $\Delta\tau_h \approx 5$ s upon an increase in the mass of water from 5 to 15 mg (see Fig. 5).These long times for the complete evaporation of drops (close to the corresponding valued for inhomogeneous drops), as well as their insignificant variations upon an increase in the mass of water, are due to the formation of the heat-insulating vapor layer [24–26] between the substrate and the drop (see Figs. 3b and 3c), which slows down the evaporation process.

The results of experiments that were performed in accordance with the technique of the first stage and depicted in Figs. 6a and 6b illustrate the effect of the increase in the area of the inclusion surface on the intensity of evaporation of an inhomogeneous drop. It should be noted that the main mechanism of phase

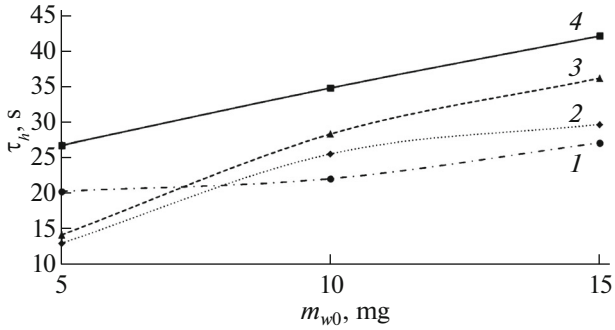

Fig. 5. Lifetimes (complete evaporation times) of water drops on the substrate (*1*) and upon complete enveloping of an inclusions with various characteristic sizes of (*2*) 4, (*3*) 3, and (*4*) 2 mm.

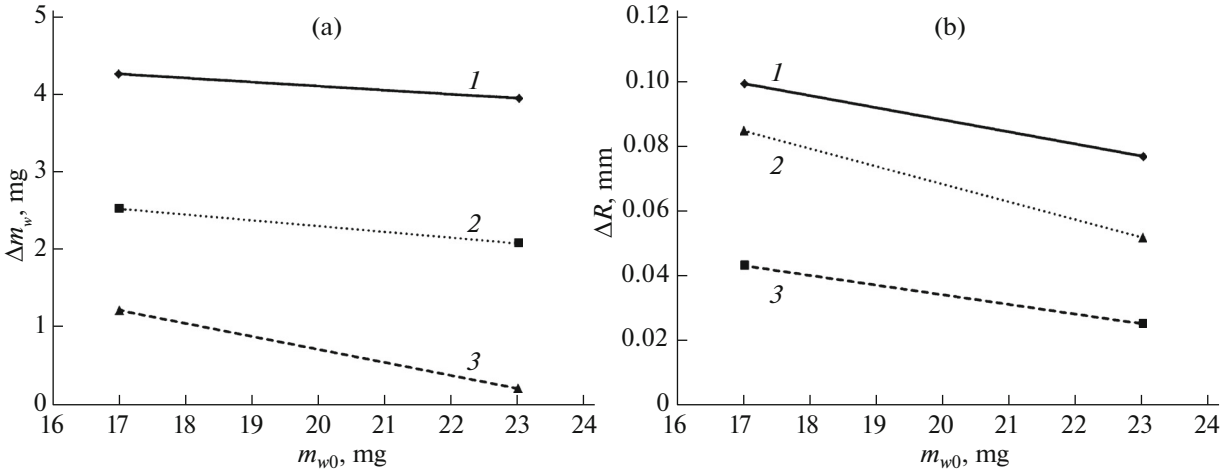

Fig. 6. Dependences of parameters (a) Δm_w and (b) ΔR on the initial mass m_{w0} of water for different shapes of inclusion: (*1*) cylinder; (*2*) cube; (*3*) parallelepiped.

transformations in this case is the evaporation from the outer surface of the inhomogeneous water drop (the formation of a vapor layer at the inclusion–water interface was not detected in the drop leaving the high-temperature medium). In contrast to experiments illustrated in Figs. 3 and 4, in the case of the short-term heating of an inhomogeneous drop (0.3–0.5 s in the regime of free fall in the channel of height 1 m), an inclusion with a smaller surface area was heated sooner and, hence, the decrease Δm_w in the mass of the liquid increased (Fig. 6a). The decrease in the mass of the inhomogeneous water drop led to a decrease in its size (Fig. 6b). Upon an increase in the initial mass m_{w0} of water, we detected a decrease in parameters Δm_w and ΔR (see Figs. 6a and 6b). This result can be explained by an increase in the time of heating the layer of liquid and, hence, the inclusion. Thus, the effect of the solid inclusion on the intensification of evaporation during short-term heating can be considered to be quite moderate.

In our experiments, convective and radiant heat exchange with gases on the drop surface played a decisive role. The corresponding heat fluxes can be determined (in the first approximation) using expressions of the form [29–31] $q_c = \alpha(T_g - T_c)$ and $q_1 = \varepsilon\sigma(T_g^4 - T_c^4)$. According to [32–34], the heat-exchange conditions on the surface of a drop can be described using the Rantz–Marshall relation $\mathrm{Nu} = 2 + 0.6\mathrm{Re}^{1/2}\mathrm{Pr}^{1/3}$. In our experimental conditions with combustion products, the values of heat-transfer coefficients α with this approach do not exceed 5–7 W/(m^2 K).

The coefficient ε for an evaporating liquid heated by a gas is determined taking into account the radiant properties of gases (combustion products) and vapors. The radiation spectrum of gases that make up the combustion products of alcohol, as well as other combustible liquids (primarily, water vapor and carbon dioxide) is characterized by so-called emission (absorption) bands that are associated with the change in the state of molecules and atoms. The main bands in the radiation spectra of carbon dioxide and water vapor are [35, 36] $\lambda_{1\mathrm{CO}_2} \approx 2.65$–$2.8$ μm, $\lambda_{2\mathrm{CO}_2} \approx 4.15$–$4.45$ μm, $\lambda_{3\mathrm{CO}_2} \approx 13$–$17$ μm, $\lambda_{1\mathrm{H}_2\mathrm{O}} \approx 2.3$–$3.4$ μm, $\lambda_{2\mathrm{H}_2\mathrm{O}} \approx 4.4$–$8.5$ μm, and $\lambda_{3\mathrm{H}_2\mathrm{O}} \approx 12$–$30$ μm. The presence in the radiation spectra of the main (emitting) components of combustion products should be taken into account in calculating the emissivity factor of the high-temperature gaseous medium. It can be calculated in accordance with the mean value of volume fractions of the corresponding components in the alcohol combustion products (the values of volume fractions of CO_2 were obtained using the gas analyzer; the volume fraction of water vapor in the combustion products was averaged in accordance with reference data [35, 36]), the optical thickness of gases, and their temperatures. It is important that water vapor is one of the main generators of radiation in the combustion products–water vapor–drop system; according to the experimental data [37, 38], its concentration in a thin surface layer can be very high. For this reason, the radiant component will only increase. Using reference data [35, 36] for the established concentrations of combustion product components (4.433% CO_2, 0.058% CO, 14.907% O_2, 0.002% NO, 0.002% NO_x, and 80.598% of other hydrocarbon components and N_2) and temperature (1100 K), the average value of coefficient ε was found to be 0.254.

In accordance with the modern concepts of phase transformations of liquids, the maximal temperature of the water drop surface (T_e) can be 370 K (boiling point of water). Numerical simulation [4, 39, 40] shows that these temperatures can be attained on the

surface of inhomogeneous drops a few seconds from the beginning of heating at a gas temperature of 1100 K.

Using these initial data, we determined the values of the convective (q_c) and radiant (q_r) heat fluxes on the drop surface as follows: $q_c = \alpha(T_g - T_e) = 5(1100 - 370) \approx 3650$ W/m^2; $q_r = \varepsilon\sigma(T_g^4 - T_e^4) = 0.254 \times 5.669 \times 10^{-8} \times (1100^4 - 370^4) \approx 20812$ W/m^2.

An analysis of q_c and q_r shows that, in experiments with moving drops (first stage in this study), the convective and radiant heat fluxes can only be comparable for high velocities of drops (exceeding 5–7 m/s). In our experiments, these conditions were not observed because experiments were carried out in free-fall conditions. In addition, an analysis of the experimental results [41–43] leads to the conclusion that the probability of the substantial transformation of the surface followed by splitting of the drop is high at these velocities.

The role of the radiant heat exchange of a liquid drop with combustion products increases due to opaque inclusions with a highly emissivity factor. Simulation [4, 39, 40] shows that 30–40% of supplied radiant energy is absorbed by the inclusion in the drop. The remaining energy is spent to heat and evaporate water on the outer (free) surface, as well as on inner interfaces between the media (at the surface of an inclusion). As a result, we can conclude that the radiant component dominates in the mechanisms of heat exchange between inhomogeneous liquid drops and high-temperature combustion products.

Additional experiments were carried out in order to estimate the difference between the complete evaporation times for water drops (with the identical initial masses) on the substrate and around an inclusion for various heating temperatures. The temperature of the combustion products was varied in the range of 300–650 K (analogously to the technique used in [40]). The main results are shown in Fig. 7.

In the range of low temperatures, the deviations of parameter $\Delta\tau_h$ can attain 35 s (Fig. 7). With increasing temperature, the deviations in the integrated evaporation parameter decreases nonlinearly (down to 5 s at $T_g \approx 650$ K). This effect indicates that, under the conditions of high gas temperatures (especially for small drops), evaporation processes in the systems under investigation can be characterized by close values of τ_h. However, the physical natures of the processes can be quite different (mainly, in the mechanisms of evaporation at the liquid–solid interfaces). In the case of moving inhomogeneous drops, the times of their residence in the high-temperature gaseous medium play the decisive role. It is this factor that determines the possibility of evaporation or boiling on the inner and outer interfaces between the media. The implementation of one or several mechanisms of phase transformations predetermines the temporal characteristics of evaporation of the liquid. With regard to practical applications, the allowance for the time of interaction of inhomogeneous liquid drops and the high-temperature gaseous medium presumes variations in the geometrical parameters of inclusions (their size and shape).

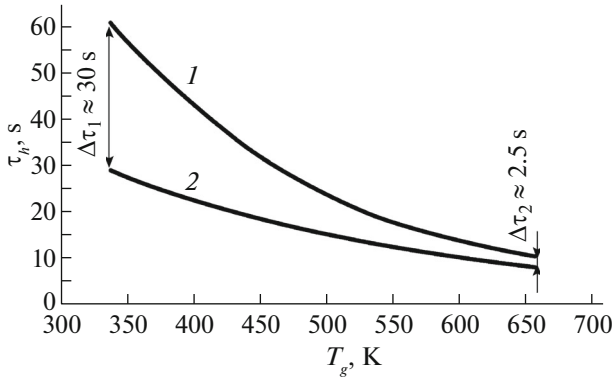

Fig. 7. Lifetimes of a water drop (of mass 10 mg) enveloping the inclusion (*1*) and on the substrate (*2*) for different gas temperatures.

Our results extend state-of-the-art concepts concerning the main regularities of evaporation and boiling of liquid drops [44–48] under the conditions of intense heat transfer. At the same time, an analysis of the main processes of the formation of the vapor layer at the liquid–solid particle interface is essential for studying the regime of boiling at the interfaces between the media in the given conditions and in the search for approaches for its intensification.

CONCLUSIONS

1. Variations in the surface area of an inclusion substantially (up to 20%) affects the characteristics of the evaporation of inhomogeneous liquid drops.

2. An increase in the initial mass m_{w0} of a water drop in the composition of an inhomogeneous water drop by even 6 mg facilitates the reduction of parameters Δm_w (down to 90%) and ΔR (to 50%).

3. It has been found that the formation of a vapor layer at the substrate–liquid interface produces a decisive effect on the lifetime of the water drop evaporating from the substrate (τ_h changes by 20% upon an increase in the initial mass of water from 5 to 15 mg).

4. The difference $\Delta\tau_h$ detected upon a change in the gas temperature shows that in the application of high-temperature gas–vapor–drop mixtures, close integrated characteristics (evaporation rates and lifetimes) of evaporation can be obtained for different positions of the solid–liquid contact zone. However, in this case, the conditions of boiling or evaporation (formation of the vapor layer, nucleation, growth, and destruction of bubbles, etc.) may differ significantly.

5. The established features of the processes considered here make it possible to predict the conditions and characteristics of phase transformations in inhomogeneous drops in high-temperature gaseous media (under various conditions of contact with inclusions and the solid surface).

ACKNOWLEDGMENTS

This work was supported financially by the grant (no. MD-2806.2015.8) from the President of the Russian Federation.

NOTATION

m_{w0}—initial mass of water on the substrate and around the inclusion, mg;

m_w—mass of water around the inclusion after the passage through the high-temperature gaseous medium, mg;

Δm_w—parameter that characterizes the decrease in the mass of a water drop, mg;

q_c and q_r—the convective and radiant heat fluxes at the surface of the drop, respectively, W/m^2;

R—radius of an inhomogeneous drop after its passage through the high-temperature gaseous medium, mm;

R_0—initial radius of an inhomogeneous drop, mm;

ΔR—parameter that characterizes the decrease in the sizes of inhomogeneous drops during evaporation, mm;

T_e—temperature of the drop surface, K;

T_g—temperature of combustion products, K;

u_g—velocity of the high-temperature gas flow, m/s;

α—heat-transfer coefficient, W/(m^2 K);

ε—emissivity factor;

σ—Stefan–Boltzmann constant, W/(m^2 K^4);

τ—time, s;

τ_h—lifetime of water drops surrounding an inclusion and on the substrate, s;

$\Delta\tau_h$—parameter that characterizes the difference in the times of complete evaporation of water on the substrate and around an inclusion, s;

Nu, Pr, and Re—dimensionless complexes (Nusselt, Prandtl, and Reynolds numbers).

REFERENCES

1. R. S. Volkov, G. V. Kuznetsov, and P. A. Strizhak, Tech. Phys. **59**, 1770 (2014).
2. V. E. Nakoryakov, G. V. Kuznetsov, and P. A. Strizhak, Dokl. Phys. **60**, 428 (2015).
3. D. Ciloglu and A. Bolukbasi, Nucl. Eng. Des. **241**, 2519 (2011).
4. R. S. Volkov, M. V. Piskunov, G. V. Kuznetsov, and P. A. Strizhak, J. Heat Transfer **138**, 1 (2016).
5. H. Kim, G. DeWitt, T. McKrell, J. Buongiorno, and L.-W. Hu, Int. J. Multiphase Flow **35**, 427 (2009).
6. A. N. Ishchenko, Voda: Khim. Ekol., No. 7, 2 (2010).
7. A. Yu. Val'dberg and K. P. Makeeva, Khim. Neftegazov. Mashinostr., No. 5, 42 (2010).
8. X. Zhou, S. P. D'Aniello, and H.-Z. Yu, Fire Saf. J. **54**, 36 (2012). doi 10.1016/j.firesaf.2012.07.007
9. M. N. Nikitin, Prom. Energ., No. 12, 37 (2010).
10. *Theory of Control over the Pelletizing of Loose Materials,* Ed. by E. A. Isaev, I. E. Chernetskaya, L. N. Krakht, and V. S. Titov (Staryi Oskol, 2012).
11. *Surface Treatment in Metallurgy and Machine Building,* Ed. by B. N. Mar'in (Dal'nauka, Vladivostok, 2011).
12. I. S. Anufriev, G. V. Kuznetsov, M. V. Piskunov, P. A. Strizhak, and M. Yu. Chernetskii, Tech. Phys. Lett. **41**, 810 (2015).
13. Yu. I. Yalamov and M. K. Kuz'min, Tech. Phys. **50**, 314 (2005).
14. R. Mollaret, K. Sefiane, J. R. E. Christy, and D. Veyret, Chem. Eng. Res. Des. **82**, 471 (2004).
15. F. Girard, M. Antoni, and K. Sefiane, Langmuir **26**, 4576 (2010).
16. H. Y. Erbil, G. McHale, and M. I. Newton, Langmuir **18**, 2636 (2002).
17. M. A. Dmitrienko, M. V. Piskunov, P. A. Strizhak, and A. A. Shcherbinina, MATEC Web Conf. **23**, 01064 (2015).
18. R. D. Keane and R. J. Adrian, Appl. Sci. Res. **49** (3), 191 (1992).
19. J. Westerweel, Meas. Sci. Technol. **8**, 1379 (1997).
20. J. M. Foucaut and M. Stanislas, Meas. Sci. Technol. **13**, 1058 (2002).
21. J. Janiszewski, Metrol. Measur. Sys. **19**, 797 (2012).
22. J. Janiszewski, Int. J. Solids Struct. **49**, 1001 (2012).
23. J. Janiszewski, Solid State Phenom. **199**, 297 (2013).
24. J. G. Leidenfrost, Int. J. Heat Mass Transfer **9**, 1153 (1966).
25. B. S. Gottfried, C. J. Lee, and K. J. Bell, Int. J. Heat Mass Transfer **9**, 1167 (1966).
26. A.-L. Biance, C. Clanet, and D. Quere, Phys. Fluids **15**, 1632 (2003).
27. N. B. Vargaftik, *Thermal Properties of Gases and Liquids. A Handbook* (Stars, Moscow, 2006).
28. Y. S. Touloukian, R. W. Powell, C. Y. Ho, P. G. Klemens, *Thermophysical Properties of Matter,* The TPRC Data Series, Vol. 2: *Thermal Conductivity—Nonmetallic Solids* (IFI/Plenum, New York, 1971).
29. V. I. Terekhov and M. A. Pakhomov, *Heat and Mass Transfer and Fluid Dynamics in Gas–Droplet Flows* (Izd. NGTU, Novosibirsk, 2009).
30. D. S. Mikhatulin, Yu. V. Polezhaev, D. L. Reviznikov, *Heat and Mass Transfer, Thermal, and Thermal–Errosion Fracture of Heat Protection* (Yanus-K, Moscvow, 2011).
31. V. V. Yagov, *Heat Exchange in Single-Phase Media upon Phase Transformations* (Mosk. Energ. Inst., Moscow, 2014).
32. W. E. Ranz and W. R. Marshall, Chem. Eng. Prog. **48** (3), 141 (1952), Chem. Eng. Prog. **48** (3), 173 (1952).

33. N. A. Fuchs, *Evaporation and Droplet Growth in Gaseous Media* (Pergamon, London, 1959).
34. V. I. Terekhov, V. V. Terekhov, N. E. Shishkin, and K. Ch. Bi, Inzh. Fiz. Zh. **83**, 829 (2010).
35. V. N. Yurenev and P. D. Lebedev, *Heat Engineering Handbook* (Energiya, Moscow, 1976), Vol. 2.
36. *Heat Calculation of Boilers: Normative Method,* 3rd ed. (TsKTI, St. Petersburg, 1998).
37. R. S. Volkov, G. V. Kuznetsov, and P. A. Strizhak, Int. J. Heat Mass Transfer **79**, 838 (2014).
38. G. V. Kuznetsov, P. A. Kuibin, and P. A. Strizhak, Teplofiz. Vys. Temp. **53**, 264 (2015).
39. O. V. Vysokomornaya, M. V. Piskunov, P. A. Strizhak, and A. A. Shcherbinina, Pozharovzryvobezopasnost **24** (7), 9 (2015).
40. G. V. Kuznetsov, M. V. Piskunov, and P. A. Strizhak, Int. J. Heat Mass Transfer **92**, 360 (2016).
41. R. S. Volkov, G. V. Kuznetsov, and P. A. Strizhak, Int. J. Heat Mass Transfer **85**, 1 (2015).
42. R. S. Volkov, O. V. Vysokomornaya, G. V. Kuznetsov, and P. A. Strizhak, Tech. Phys. **60**, 1119 (2015).
43. R. S. Volkov, A. O. Zhdanova, G. V. Kuznetsov, and P. A. Strizhak, Tech. Phys. **60**, 1443 (2015).
44. Yu. I. Yalamov and N. N. Golikova, Tech. Phys. **51**, 173 (2006).
45. E. V. Anokhina, Tech. Phys. **55**, 1107 (2010).
46. S. S. Sazhin, A. E. Elwardany, P. A. Krutitskii, G. Castanet, F. Lemoine, E. M. Sazhina, and M. R. Heikal, Int. J. Heat Mass Transfer **53**, 4495 (2010).
47. S. S. Sazhin, A. E. Elwardany, P. A. Krutitskii, V. Depredurand, G. Castanet, F. Lemoine, E. M. Sazhina, and M. R. Heikal, Int. J. Therm. Sci. **50**, 1164 (2011).
48. S. S. Sazhin, P. A. Krutitskii, I. G. Gusev, and M. R. Heikal, Int. J. Heat Mass Transfer **54**, 1278 (2011).

Translated by N. Wadhwa